Reduced shrinkage of sol–gel derived silicas using sugar-based silsesquioxane precursors†

Yang Chen, Zheng Zhang, Xihua Sui, John D. Brennan and Michael A. Brook*

Received 28th February 2005, Accepted 25th May 2005
First published as an Advance Article on the web 22nd June 2005
DOI: 10.1039/b502959g

Monolithic siliceous materials were prepared, using sol–gel based methods, from mixtures of trifunctional silanes based on sugar lactones, including silyl-modified gluconamide GLS and maltonamide MLS, and a tetrafunctional silane derived from glycerol. The tri- and tetrafunctional compounds cured at different rates, which led to an enhanced presence of sugar moieties at the external surface of the pores in the monoliths. The resulting silicas exhibited dramatically reduced degrees of shrinkage (<10%) when compared to silica monoliths prepared in the absence of trifunctional silanes (up to 85%). The sugars also alter the morphology of the material, with significant reductions in both micropore volume and surface area for materials containing GLS. The reduced shrinkage, presence of sugars on the silica surface, and altered morphology are likely to be important factors in providing such materials with the ability to stabilize entrained proteins.

Introduction

The use of sol–gel processing methods provides an exceptional degree of control over the composition and morphology of silicate materials. Thus, total porosity, pore size and shape, regularity of pore distribution, *etc.*, can be manipulated using a variety of starting materials, reaction conditions and dopants.[1] Many of these conditions, however, are incompatible with the incorporation of fragile compounds such as biomolecules, proteins in particular. Either the synthetic conditions are damaging to protein structure (*e.g.*, pH conditions, the presence of denaturants such as ethanol) or the final curing conditions require elevated temperatures. Furthermore, many materials undergo significant changes as a result of aging (*i.e.*, shrinkage, pore collapse, alterations in internal polarity and water content, *etc.*) that lead to poor long-term stability of entrapped proteins. Thus, it is of interest to prepare improved materials that can incorporate active biomolecules in silica matrices to create materials that can serve as biosensors, immobilized enzyme reactors or affinity chromatography supports.[2–7]

Several strategies have been developed to mitigate the effects of aging on sol–gel derived silica. Gill and Ballesteros described poly(glycerylsilane)s (PGS) as precursors for silica that exhibited reduced shrinkage and increased pore sizes.[8] Brook *et al.* have reported a series of sugar, sugar alcohol, oligo- and polysaccharide-derived silanes as precursors to protein compatible silicas.[9,10] The use of these latter compounds as starting materials, particularly diglycerylsilane (DGS) and monosorbitylsilane, reduced the normally high shrinkage levels during drying of TEOS-derived silica (up to 85% shrinkage) to as low as 50% over 2 months under ideal conditions. While this represents a significant improvement in the sol–gel synthesis, it is insufficient when the protein-doped gels are to be used in applications such as chromatography, for which void spaces resulting from shrinkage or cracking are significantly detrimental to performance. In addition, while DGS based materials provided improved stability for many proteins relative to TEOS based materials, there were still significant losses in activity for many proteins with aging, and a complete lack of activity for other proteins.[11]

One method that was recently reported for creating highly biocompatible sol–gel derived materials was to include trifunctional silanes bearing covalently bound sugars into DGS derived silica to produce sugar-modified silica. Sugars are known to be stabilizing toward proteins,[9,12] and indeed sugar-modified materials were shown to be amenable to entrapment of fragile enzymes including urease, Factor Xa, luciferase and Src kinase.[13] The contributing factors for protein stabilization included the presence of the glycerol, and absence of denaturants, lower monolith shrinkage and higher water retention.[13] More recent studies of entrapped human serum albumin (HSA) demonstrated that initial conformation, accessibility to external analytes, thermal stability, long-term stability and degree of ligand binding to HSA were best in DGS-derived materials that contained covalently tethered gluconamidylsilane (GLS) moieties relative to unmodified DGS-derived materials, TEOS or TEOS–GLS-derived materials. Measurement of protein rotational dynamics showed that entrapment led to an immediate loss of global motion in all materials. However, the restriction of motion was most dramatic in GLS doped materials, suggesting preferential interactions of the protein with the sugar coated surfaces.

Trifunctional silanes form silsesquioxanes upon hydrolysis,[14,15] which generally show a lower degree of crosslinking

Department of Chemistry, McMaster University, 1280 Main St. W., Hamilton, ON, Canada L8S 4M1. E-mail: mabrook@mcmaster.ca; Fax: +1 905 522 2509; Tel: +1 905 525 9140 ext. 23483

† Electronic supplementary information (ESI) available: Figures of ATR FT-IR, FT-IR, ^{13}C NMR and ^{29}Si NMR data for samples **3**–**5** and **8**–**10**. See http://dx.doi/10.1039/b502959g/

than materials derived from tetrafunctional silanes. In addition, trifunctional silanes are frequently used as surface modifying materials, as coupling agents or adhesion promoters.[16] In cases where trifunctional and tetrafunctional silanes are co-hydrolyzed and condensed, the trifunctional materials will generally cure more slowly than the tetraalkoxysilane counterparts, depending on the specific kinetics at the pH used for the hydrolysis/condensation sequences.[17,18] As a result, the non-hydrolyzed group on the trifunctional silane is ultimately expected to be preferentially located on the exposed surfaces of pores and microchannels in the resulting siliceous material, which would change the nature of the interactions between these surfaces and the entrapped biomolecules.

In order to test this hypothesis, and with the desire to develop matrices suitable for protein entrapment, we have prepared materials containing mixtures of trifunctional silanes based on sugars [GLS and the analogous maltonamidylsilane (MLS)],[19–21] and tetrafunctional silanes based on DGS, and have examined the morpohology, shrinkage, surface composition, shrinkage and retention of water by such materials. The material properties are related to the protein stabilizing properties of the materials, providing new insights into why such materials are capable of maintaining protein activity.[22]

Results

Preparation of coupling agents

Two classes of coupling agents based on saccharides were prepared, those derived from a mono-GLS (from gluconamide), and a disaccharide MLS (from maltose), respectively (Table 1). Although a variety of approaches exist to graft sugars to silanes, we chose to modify the anomeric hemiacetal centre at the terminus of the saccharidic chains. Oxidation of either of the sugars,[23] normally performed with iodine,[24] converts the anomeric hemiacetal into the lactone that can then be opened by an amino-modified alkoxysilane to produce a sugar-modified coupling agent.[21] These materials were characterized by standard spectroscopic techniques including IR, ^{13}C NMR and MS as summarized in Scheme 1. It should be noted that while both sugars studied are reducing sugars, the general protocol described herein should be amenable to both reducing and non-reducing sugars.

Silica–silsesquioxane composites

Unlike many trifunctional silanes based on ethoxy and methoxy groups, the compounds GLS and MLS are soluble in water. Also unlike normal organically modified trialkoxysilanes,[16] the sols of neither of these compounds alone gelled, even after 6 months.

Table 1 ^{13}C NMR, FT-IR and ESI spectral data of gluconamide silane and maltonamide silane

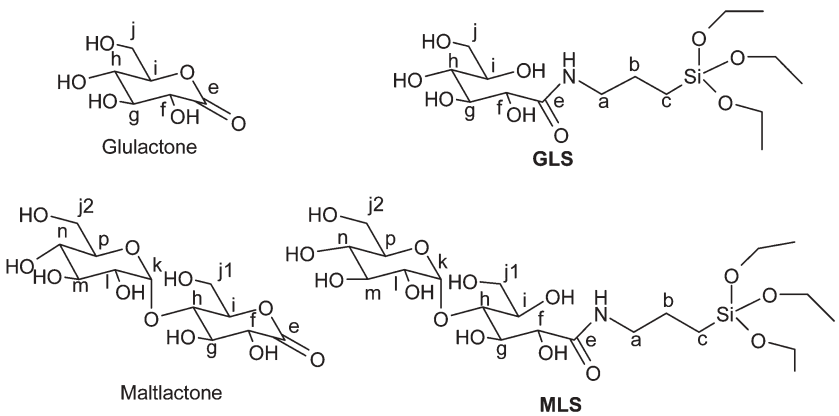

Compound		Glulactone	GLS	Maltlactone	MLS
^{13}C	Carbonyl	e 172.6	e 172.9	e 172.9	e 172.6
	Anomeric			k 100.5	k 101.4
	Methyne	f 81.9	f 74.2	f, g, i, l, m, p	f, g, i, l, m, p
		g 72.0	g 72.1	70.5–73.5[a]	72.5–73.8[a]
		h 68.4	h 70.7	h 80.4	h 80.6
		i 74.3	i 73.0	n 69.8	n 69.8
	Methylene	j 60.8	j 64.0	j_1 61.0	j_1 61.3
			a 41.5	j_2 61.3	j_2 63.4
			b 23.3		a 41.3
			c 7.8		b 23.4
					c 7.8
	OCH_2CH_3		18.7 ~ 18.9		18.4 ~ 19.1
			58.3 (overlapped)		58.3[a]
IR (neat, KBr) ν(C=O) cm^{-1}		1728	1646	1747 (δ-lactone)	1646
MS (ESI) *m/z*			422.2 (100)(M + Na)$^+$		584.3 (30)(M + Na)$^+$
			400.2 (15)(M + 1)$^+$		562.4 (20)(M + 1)$^+$

[a] A series of overlapped peaks.

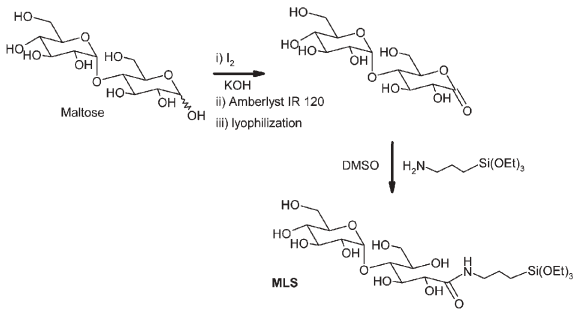

Scheme 1 Preparation of sugar coupling agents, shown for MLS.

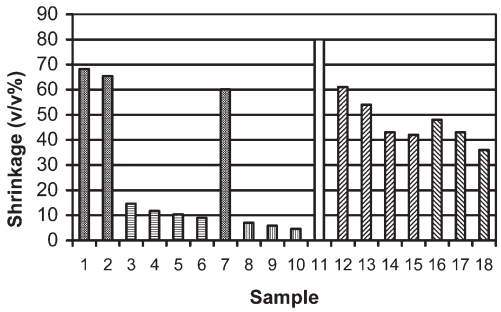

Fig. 1 Shrinkage data of samples **1**–**18** over 45 d. DGS (**1**), DGS + GLS (**3**–**6**), DGS + MLS, TEOS (**11**), TEOS + GLS (**12**–**15**), TEOS + MLS (**16**–**18**). Recipes for these monoliths are provided in Tables 2–4.

A series of gels derived from the co-hydrolysis of DGS with compounds GLS or MLS, respectively, led to organically modified silicas possessing very different properties than silica derived from DGS alone. Curing kinetics for the composites depended upon the ratio of starting materials. There was a trend to slower curing with an increase in the proportion of the trifunctional component (Table 2). For practical reasons, the amount of compounds GLS had to be limited to about 75 mol% (75 mol% GLS ≈ DGS : GLS 1 : 6 *w*/*w*), and MLS to about 40 mol%, above which curing did not occur within about 1 week. In all cases, optically clear monolithic silsesquioxane-modified silicas resulted after aging for one week post gelation.

The physical behavior of the resulting silica–silsesquioxane composites was studied. The most significant change between the monolithic silicas derived from DGS alone, and those that also included sugar-based coupling agent GLS and MLS, was the degree of shrinkage of the siliceous products. Shrinkage is directly linked to the degree of hydration of the monolith and the presence of sugars in the gel. Unwashed samples **1**, **3**–**6**, and **8**–**10**, which still contained entrained glycerol, showed no shrinkage over 45 d in air.[25] Washed samples (see the Experimental section), which contained the sugar (derived from GLS and MLS) but not glycerol (see TGA results below), similarly did not shrink if stored under water in closed containers over 6 months. Normally, shrinkage of washed samples of DGS-derived gels, when allowed to rest in an open environment (*i.e.*, not under water), occurs to a level of up to approximately 65% (see sample **1**, Fig. 1), much less than TEOS-derived gels, which shrink approximately 85%.[9] By contrast, the incorporation of the sugar-modified trifunctional groups GLS or MLS into a DGS gel dramatically reduces shrinkage of the modified silicas, in some cases by an order of magnitude to less than 10%, after drying in air over the same lengthy (45 d) time period (samples **3**–**6**, **8**–**10**, Fig. 1).

For comparison, the effects of GLS or MLS on shrinkage in TEOS gels were examined (Fig. 1, **11**–**18**). After washing and drying for 57 d, there was a marked decrease in shrinkage (about 2×) over TEOS alone (80%), **11**, but the degree of shrinkage in the TEOS–GLS material (42%) was still significantly greater than was observed with the combination of DGS and the sugar-based coupling agents (*e.g.*, compare TEOS–GLS sample **16** 42% shrinkage *vs.* DGS–GLS sample **6** 6% shrinkage, Fig. 1). This demonstrates that glycerol (in DGS) and the saccharidic amides (from GLS or MLS) act cooperatively to reduce shrinkage.

The reduced shrinkage of these monoliths could be a consequence of the entrained sugars, and/or the accompanying water. Thermogravimetric analysis (TGA) was utilized to better understand the degree to which GLS and MLS and the glycerol product of hydrolysis were physically and chemically constrained within the monolith. A comparison was initially made between unwashed gels and those that had been first washed with water to remove ungrafted material.

All the samples contained significant amounts of water, as is to be expected from the presence of hygroscopic sugar-containing moieties. For example, the TGA of an unwashed sample **1** showed loss of about 15% weight of water and a further 12% weight change associated with loss of glycerol above 150 °C (Fig. 2). After washing with water, the same sample **1** had little residual weight loss (2.7%) after the temperature was raised to 150 °C (data not shown). These observations confirm that most of the glycerol formed by hydrolysis of DGS is initially available in accessible micro- or mesopores, or channels connecting the two, but can then be easily removed by washing.

The kinetics of water loss were investigated from samples **1** and **4** (samples were washed, but not freeze dried). TGA, at fixed temperature of 40 °C in air over an experimental period of 75 min (Fig. 3), showed surprisingly linear drying kinetics for physically absorbed water.[26] Sample **4**, containing grafted

Table 2 Preparation of TQ resins

Sample	Ratio of DGS : GLS (*w*/*w*)	Gelation time/min	Aged/d
1	1 : 0	10	7
2a	DGS : sorbitol, 4 : 1	60	7
3	4 : 1	65	7
4	3 : 1	70	7
5	2 : 1	90	20
6	1 : 1	90	20
Sample	Ratio of DGS : MLS (*w*/*w*)	Gelation time/min	Aged/d
7[b]	DGS : maltose, 16 : 1	55	7
8	16 : 1	60	7
9	8 : 1	70	7
10	4 : 1	70	7

[a] This model system contained only DGS and sorbital, a sugar analogue of GLS that cannot covalently bind into the matrix. [b] This model system contained only DGS and maltose, a sugar analogue of MLS that cannot covalently bind into the matrix.

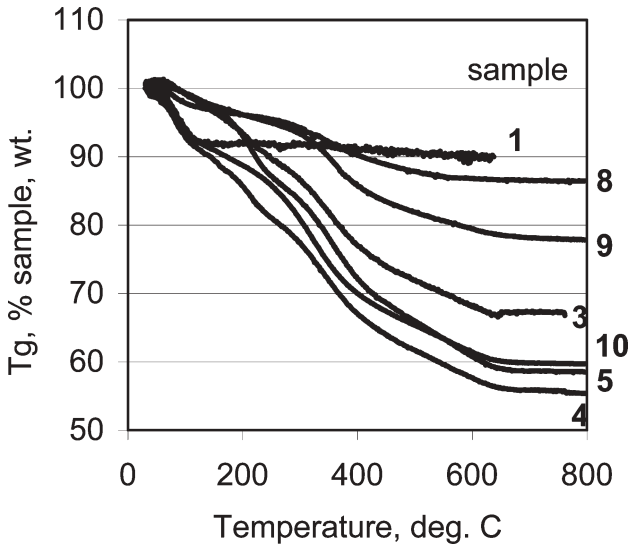

Fig. 2 TGA of unwashed samples **1** (after washing, the weight loss was 2.7%), **3**–**5**, and **8**–**10**.

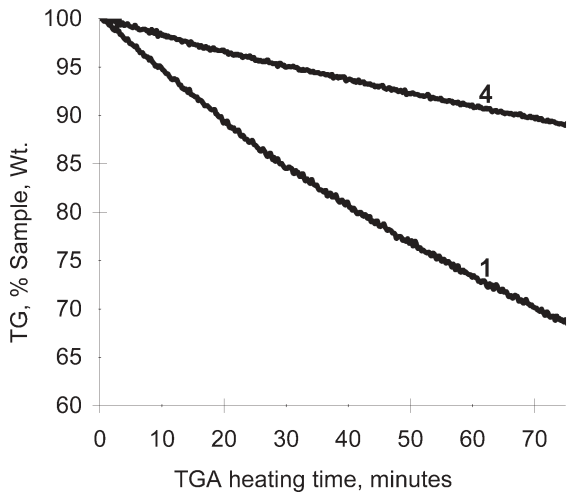

Fig. 3 TGA comparison of the drying kinetics of wet samples **1** and **4** by measured weight loss at 40 °C over 75 min.

saccharide that holds tenaciously onto water, showed slower release kinetics.

To normalize the degree to which all samples were hydrated, and also to remove ungrafted sugars, the remaining samples were allowed to age for 7 d, were ground up, washed with water (see experimental section), freeze dried for 2 d and characterized by TGA.

Silica gels containing grafted GLS and MLS, both of which are hygroscopic, showed loss of significant amounts of water on heating. Surprisingly, however, there was no correlation between the sugar content and the amount of entrained water in the monoliths: after washing, all monoliths exhibited weight losses due to water of 5–10%.

Once bonded into the matrix, sugar moieties derived from GLS or MLS could not be cleaved by normal hydrolysis and/or removed by washing. After washing the gels to remove residual, ungrafted material including glycerol and ungrafted GLS and MLS, respectively, the presence of the residual

Table 3 TGA data on TEOS and sugar–TEOS gels

Sample	Sugar–TEOS (mol %)		TGA data (weight loss, %)
11	TEOS		2.15
12	GLS–TEOS	5	10.3
13		10	16.9
14		15	25.7
15		20	31.5
16	MLS–TEOS	5	11.2
17		10	27.9
18		15	37.7

carbohydrates in proporation to their concentration in the sol was clearly demonstrated by TGA (Table 3). Significantly more organic material could be pyrolyzed from samples **3**–**5** and **8**–**10** (10–38% wt, Fig. 2, Table 4) than from the silica derived solely from DGS. Colour (yellow → dark brown) evolved in samples **3**–**5** and **8**–**10** starting about 200 °C due to a caramelization of the grafted sugar. In the case of TEOS sols **11**, to which the sugar-based coupling agents were added (**12**–**18**, Fig. 2), residual sugars were also present in the monolith in proportion to their composition in the sol (Table 3).

The difference between the theoretical and measured weight loss provides guidance as to the efficiency of incorporation of GLS and MLS during condensation (samples **3**–**5** and **8**–**10**), (Table 4). These values were confirmed by combustion elemental analysis data of the gels (Table 5). The quantity of nitrogen, in particular, is diagnostic of the amount of saccharide present. The efficiency of sugar incorporation, from about 30–70%, was related to a degree both to the type of

Table 4 Thermogravimetric analyses of samples **1**, **3**–**5**, **8**–**10**

Sample	Ratio of DGS : Sugar coupling agent (w : w)	Theoretical weight loss (%)[a]	Weight loss by TGA	Efficiency of T incorporation[b]
1	100 : 0	0.0	2.17	—
3	80 : 20 (GLS)	50.0	29.9	60
4	75 : 25 (GLS)	55.4	38.2	69
5	66 : 33 (GLS)	62.1	31.5	51
8	94 : 06 (MLS)	33.4	10.3	31
9	89 : 11 (MLS)	48.5	19.7	41
10	80 : 20 (MLS)	62.7	33.4	53

[a] Assuming all added GLS or MLS is incorporated the monolith and C,N,H are lost as gaseous byproducts. [b] Assuming alkoxysilane hydrolysis is complete, and the only residual source of carbon arises from the saccharide residues in GLS or MLS.

Table 5 Elemental analyses of sample **3**–**5**, **8**–**10**

Sample	C (%)	N (%)	Sugar based on Ca (wt%)	Sugar based on Na (wt%)
3	14.87	1.70	39.7	35.0
4	14.97	1.73	39.9	35.6
5	16.76	1.98	44.7	40.7
8	6.13	0.54	15.3	17.3
9	9.65	0.51	24.0	16.3
10	13.18	0.94	32.8	30.1

[a] Using the molecular formula for sugar as sugar-C=O–$NH(CH_2)_3SiO_{3/2}$. The amount of residual unhydrolyzed alkoxysilane groups is reflected in the difference between the N and C values and, as can be seen, is rather limited.

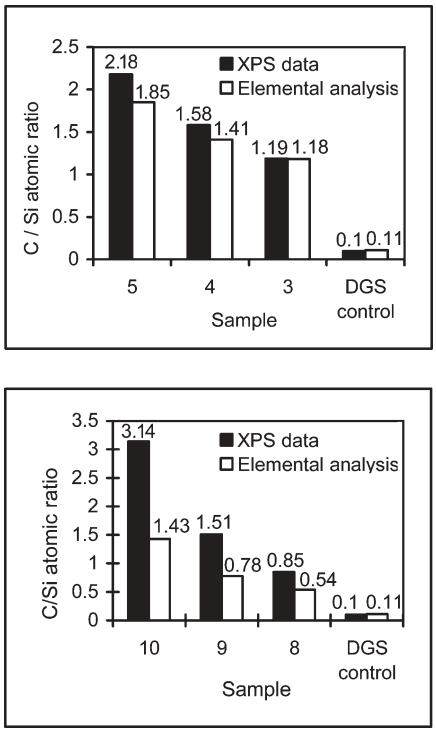

Fig. 4 XPS and elemental analysis results for powder samples **3**–**5**, and **8**–**10**.

T-functional silane, GLS *vs.* MLS, and their respective concentration in the sol (Table 4).

It was initially unclear whether the T units derived from compounds GLS and MLS were homogenously dispersed throughout the modified silica, located in domains within the silica, or were located primarily on the internal pore and microchannel surfaces. Dried and ground samples of the monoliths were examined by XPS to assess the nature of the surface at boundaries. Fig. 4 shows the XPS results, presented as the C/Si atom% ratio, for powdered samples **3**–**5** (prepared from DGS with increasing proportions of GLS) and **8**–**10** (prepared from DGS with increasing proportions of MLS) at takeoff angles of 90°. These data represent the elemental composition of the uppermost 50–100 Å of the exposed surface, and can be compared with elemental analysis results by combustion (Table 5), which represents the constitution of the entire sample. The higher carbon : silicon atomic ratios in the XPS than in the combustion analysis data are consistent with exposed siliceous surfaces that are enriched with the sugar-based coupling agents.

The presence of the bound sugar coupling agents into the monolith *per se* was demonstrated by both ^{29}Si and ^{13}C CP-MAS NMR spectra, which reports on the bulk sample. The increased concentration of the saccharides at the air interface was demonstrated by ATR FT-IR. The latter, in particular, is diagnostic because of the amide linkages that appear in the region between 1650 and 1700 cm^{-1} (refer to the electronic supplementary information). The resonances from sugar fragments of the trifunctional component in the ^{13}C CP-MAS NMR spectra of **3** and **10**, respectively (Table 6, also see the supplementary information), are comparable to those

Table 6 Solid-state ^{13}C and ^{29}Si CPMAS NMR spectral data of sample **3** and **10**

Sample	^{13}C, δ/ppm)	^{29}Si, δ/ppm
3	9.8, 22.8, 41.9, 63.4, 72.7, 174.5	−57.4, −66.1, −92.9, −101.2, −110.5
10	9.3, 22.2, 41.9, 63.4, 72.9, 102.6, 174.8	−57.9, −67.2, −92.6, −101.4, −109.8

Table 7 Surface characteristics of monoliths prepared with GLS, and MLS, respectively (see also the supplementary information for pore size distributions)

Sample	Ratio of DGS : sugar coupling agent w : w	Surface area/ m^2 g^{-1}	Total pore volume/ cm^3 g^{-1}	Average pore diameter/nm
1	100 : 0	635.0	0.467	2.9
3	80 : 20 (GLS)	43.4	0.035	3.2
4	75 : 25 (GLS)	3.3	0.006	7.2
8	66 : 33 (GLS)	362.7	0.661	7.3
9	94 : 06 (MLS)	332.5	0.528	6.4
10	89 : 11 (MLS)	18.9	0.023	5.0

found in the solution (DMSO) ^{13}C NMR spectra of the starting materials (Table 1), while the resonances around 18.8 and 58.3 ppm assigned to ethoxy groups disappeared following hydrolysis and condensation.

In the ^{29}Si CP-MAS NMR spectra of samples **3** and **10**, respectively (see the supplementary information), the well-known resonances of Q^2, Q^3, and Q^4 from the monolithic silica gel are accompanied by T^2 and T^3 groups in the −57 to −66 ppm range for sample **3**, and −58 to −67 ppm for sample **10**, respectively. These data are consistent with the formation of Si–O–Si linkages between sugar-based trifunctional silane and the underlying silica. That is, the monoliths are comprised of QT resins that have a higher abundance of T groups at the surface than within the structure.

The monoliths were further characterized by nitrogen absorption measurements. Monoliths prepared from DGS alone had much higher surface areas and total pore volumes than any of those prepared from recipes that included GLS (Table 7). MLS affected the system quite differently. The average pore diameter was changed in an unanticipated manner: at low concentrations, the pores and the total pore volumes are larger than monoliths prepared from DGS alone. However, with increasing concentrations, the average pore size dropped.

Discussion

Under carefully controlled conditions, trifunctional silanes can be hydrolyzed to give a series of well-defined regular prisms with Si–O–Si edges. The best known of these are the polyhedral silsesquioxanes (POSS),[27] as exemplified by T_8 derivatives (*e.g.*, T_8^{Cy} Scheme 2), a variety of which is now commercially available. More generally, however, trifunctional silanes are used to generate amorphous organofunctional layers on surfaces, where they function as "coupling agents" or "adhesion promoters".[16] With some notable exceptions,[28] it is very difficult to prepare monolayers on surfaces. Commercial applications also exist for trifunctional resins.[29]

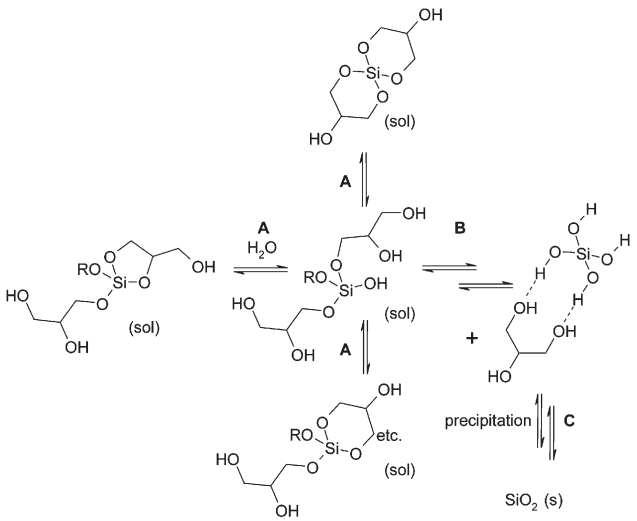

Scheme 2 Examples of polyhedral silsesquioxanes.

The relationship between the chemistry of tetrafunctional and trifunctional silanes is key in determining the resulting monolith properties. The sugar-derived trifunctional silanes GLS and MLS did not hydrolyze and cure effectively on their own: too many polyol groups are present in the sol. In the case of DGS : GLS or DGS : MLS mixtures, sols formed from mole ratios of DGS : GLS of less than 1 : 3 similarly did not lead to curing within one week.

"Normally", tetraalkoxysilanes undergo an efficient series of pH sensitive hydrolysis and condensation reactions leading to silica.[1] The term "normally", however, almost always refers to monofunctional alkoxysilanes such as $Si(OEt)_4$, TEOS and $Si(OMe)_4$, TMOS. The presence of polyols changes the cure behavior of silica sols. The hydrolysis and gelation of TEOS in the presence of glycerol greatly retards the rate of gelation.[10] DGS, constituted directly from the key elements—a tetraalkoxysilane and glycerol—undergoes curing even more slowly. This demonstrates that the presence of a polyol is not the only feature affecting curing: the proximity of the polyol to the silicon center, as in DGS, retards the gelation process.

It has been previously proposed that the presence of chemically bound or free sugars distorts the normal hydrolysis/condensation equilibria of alkoxysilanes.[10] Two factors affect this change in equilibrium. First, many more nonproductive nucleophiles are present in the sugar sol. A complex cascade of intramolecular and intermolecular nucleophilic substitutions can occur (Scheme 3a), in a sugar syrup, to compete with the hydrolysis and condensation reactions that

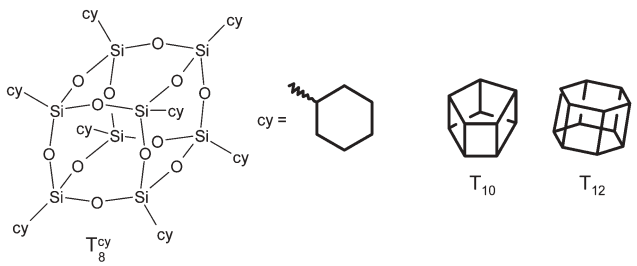

Scheme 3 Model hydrolysis/condensation reaction scheme for DGS.

ultimately lead to silica (Scheme 3b–c). Second, and perhaps more important, any polyol-containing silane moiety will be much more soluble in water than silicon species derived from monofunctional alcohols and siloxane linkages. As a result, the essentially irreversible precipitation reaction of silica is at least retarded and, in the limit, completely suppressed (Scheme 3a–b is favored over 3c). The presence of bound and unbound sugars may control the reaction in additional ways, including increasing the viscosity (retarding the rate of substitution), and sequestering water (which favors silanols over disiloxanes). Nature uses this tactic of polyol concentration to control silica formation in diatoms, plants and other organisms: sugar or catechol-rich domains sequester silicon as polyol complexes to prevent silica formation until desired, at which point, water is added to reestablish the normal equilibrium.[30,31]

The hydrolysis and condensation reactions leading to monolith formation are solution equilibria upon which is superimposed a heterogeneous equilibrium between soluble species and the insoluble silica ultimately formed. Unlike TEOS, which undergoes primary particle formation, and then particle aggregation, the precipitation of DGS can be controlled, and limited to the formation of nanoparticles because of the enhanced solubility of the DGS-derived materials.[32] The glycerol in DGS thus changes not only the equilibrium cure chemistry, but also the subsequent surface chemistry of colloidal silica materials.

The addition to a DGS sol of trifunctional compounds based on the sugar lactones GLS or MLS similarly and further significantly changes the behavior of the resulting cure processes and the characteristics of the final material. Their presence increases the load of saccharidic materials that, for the reasons enunciated above, suppress gelation. First, the presence of free or complexed (as alkoxysilanes) bidentate or multidentate alcohols slows the reaction progress. This can be seen in the efficiency of gelation; the curing reaction is retarded with increased amounts of the sugar amide in solution (Table 2, Scheme 3a). While free sugars can retard curing (Table 2, entries 2 and 6), the sugar-based alkoxysilanes are more effective at reducing the rate of gelation at a given concentration, presumably because they are directly and, in the case of GLS or MLS, irreversibly linked into the evolving matrix.

A comparison of the two alkoxysilanes GLS or MLS shows that differences exist between the two that extend beyond the simple presence of the extra sugar moieties in the latter case. Even at comparable loadings, based on saccharide units, the efficiency of incorporation was lower in the latter case (Table 4). To understand the origin of this, one must consider both the local and global concentration of saccharides. Adding free saccharides to any of the sols reduces the rate of gelation, by pushing the equilibrium reaction towards starting materials (Scheme 3). Different silicon species will be affected differently by the proximity of sugars. Tetrafunctional silicon atoms, such as those derived from DGS, exhibit reduced reactivity when the sugar is chemically bound to the silicon, rather than when simply in solution nearby (*e.g.*, TEOS + glycerol). In the case of GLS or MLS, the silicon can never escape the sugar. Thus, these materials will always be less reactive than tetrafunctional silanes. The effect of the local sugar concentrations is manifested in the much lower reactivity

of MLS than GLS, which results in a much lower capacity to be chemically bound into the monolithic TQ silica gel.

The addition of the trifunctional coupling agent to the tetrafunctional silane starting material also impacts on the surface chemistry of the resulting gel: even at much lower loadings in the sol, much more MLS was found at the silica surfaces than GLS (Fig. 1). The pH profiles of hydrolysis/condensation for tri- and tetrafunctional silanes follow similar, but not identical trends. It had been anticipated that the trifunctional silanes would undergo hydrolysis/condensation more slowly, based on the work of Osterholz and Pohl.[33] That is, sequential curing would take place. Initially, DGS would undergo hydrolysis and condensation reactions. MLS and GLS would later on begin to participate in the process and, towards the end, much higher levels of the sugar coupling agents would reside at the surface (Fig. 4). A corollary of this proposal is that the concentration of MLS and GLS would gradually increase in the sol and on the evolving gel surface over time such that, at higher concentrations further reaction will be suppressed. This view is supported by the inability to entrain all the sugarsilane coupling agents in the gel and also explains the observation that the situation in this respect is worse with MLS than with GLS: the former intrinsically cures less effectively into the silica structure and much of it will eventually be washed, unreacted or only partly reacted, from the monolithic gel.

The more significant difference observed upon adding modified trifunctional silanes GLS or MLS to the siliceous precursor, DGS,[9] is the dramatic reduction of shrinkage in the gel (Fig. 1). However, the ultimate degree of shrinkage is also strongly dependent on the nature of the tetrafunctional precursor. For comparable degrees of GLS or MLS incorporation, DGS-based gels shrank much less than TEOS derived gels: DGS 68%; TEOS 80%; DGS–GLS 10%; TEOS–GLS *ca.* 40% (Fig. 1). Two issues thus need to be addressed: the differences in shrinkage engendered by the use of DGS *vs.* TEOS, and the origins in the decrease in shrinkage when GLS or MLS are present in the sol.

Unlike the case with TEOS or DGS alone, washing a formed monolith with water cannot remove the sugars associated with GLS or MLS; they are covalently linked into the matrix, preferentially at the water-exposed interfaces. The water associated with these sugars can assist in plasticizing the monolith and, by holding onto the water, resist the evolution of capillary forces that normally occur on drying. Moreover, the addition of GLS or MLS to DGS sols leads to significant decreases in total available surface area (in non-thermally treated silicas). One explanation for this change is a loss of micropores which, if correct, would mean a dramatic reduction in the evolving capillary forces. This proposition is strongly supported by the significant loss of total surface area when GLS is present in the sol: it does not address the characteristics of the MLS-containing materials, which are currently under further investigation. Thus, the decrease in shrinkage could thus be associated both with better plasticization and an overall reduction of the magnitude of the forces responsible for shrinkage in the first place.

This explanation does not address the changes engendered by changing the alkoxygroup of the tetrafunctional silane from ethoxy to glyceroxy: TEOS gels shrink significantly more than DGS-based gels, even in the presence of additional entrained sugars derived from GLS or MLS. This likely arises from morphological differences between monoliths derived from the two tetraalkoxysilanes, which arise from different rates of curing in DGS/GLS (or MLS) sols *vs.* TEOS–GLS (or MLS) sols. Such differences arise from the change in equilibrium when sugars are present and, in unwashed samples, are exacerbated in the base of TEOS-derived monoliths by the rapid loss of ethanol through evaporation. This can lead to significant pore collapse, which will not occur when the non-volatile glycerol leaving group is present.

TEOS hydrolyses, essentially irreversibly, to give silanols and ethanol, which can then diffuse away from the reactive centre. Based on local viscosity, local water concentration, or adventitious non-productive nucleophiles, there should be no retardation of the rate. By contrast, as shown in model form in Scheme 3, DGS is fundamentally less efficient at condensation. By virtue of the covalent linkage to the saccharide groups, curing occurs even more slowly in the presence of GLS or MLS: as noted above, neither will cure independently, they must be co-constituents with tetrafunctional silanes in order to gel.

The differences in shrinkage between gels containing GLS or MLS derived from TEOS or DGS, respectively, are thus related to the differences in curing of the tetrafunctional and trifunctional silanes. TEOS will cure much more rapidly than either GLS or MLS leading to gel structures comprised of local domains of high silica content, coated with sugar rich layers derived from GLS or MLS (core shell structures). While the sugars are hygroscopic, the morphology is such that they reduce the shrinking on only a small part of the monolith. By contrast, the rates of cure of DGS and GLS or MLS, respectively, are much closer. As a consequence, there is preferential concentration of the slower curing coupling agents at the surface, but they also exist throughout the matrix where they can act as a barrier to micropores (or an agent that suppresses their formation) and as hydrated plasticization agents (ripple structure).

In addition to the consequences of shrinkage, the presence of the sugarsilane coupling agents completely changes the nature of the siliceous surface. Dramatic losses in available surface area (by nitrogen adsorption, Table 7) accompany the presence of sugar at the interface. Much more important, however, for the ultimate purpose of these monoliths, is the presentation of sugar moieties at the water interface to aid in stabilizing entrapped proteins. When proteins are present, there is a direct correlation between the lifetime of entrapped enzymes and the degree of shrinkage of the gel. Sugars are known to be stabilizing environments for proteins.[34,35]

These monoliths take advantage of sugar chemistry in a variety of ways: (i) the sugars lead to competitive curing rates between tetra- and trifunctional silanes, (ii) the resulting monoliths have sugars throughout the matrix, but preferentially at interfaces, (iii) this morphology leads to dramatically reduced shrinking, and, (iv) the surface is enriched in sugars. The latter two factors strongly contribute to enhanced stability of proteins when trapped in a silica material derived from DGS and GLS or MLS.[13,36] In particular, the presence of sugars at

the surface alters the propensity for electrostatic adsorption of proteins to the silica,[22] while at the same time presenting a biocompatible environment that may play a role in altering the hydration state,[34] and hence the dynamics,[22] of the protein. Ultimately, this leads to better long-term stability of the entrapped proteins.

Conclusion

Siliceous materials (TQ resins) were prepared using sol–gel techniques from the tetrafunctional silane DGS and trifunctional silanes based on sugar lactones. Comparison of carbon : silicon atomic ratios in the XPS and elemental analyses demonstrated that, under the conditions used, trifunctional sugar-based silane coupling agents are primarily covalently bound to the solvent exposed surface of the siliceous material. The additional use of the sugar-based, trifunctional silane coupling agents, in addition to tetrafunctional silanes, led to significantly less shrinkage of the resulting crosslinked siliceous gels and the controlled modification of the internal surfaces.

Experimental

Materials and methods

D-Gluconolactone (glulactone), D-maltose monohydrate, iodine, silver carbonate, 3-aminopropyltriethoxylsilane and anhydrous methyl sulfoxide (Aldrich Chemical Co.) were used as received. Diglycerylsilane DGS was prepared as previously reported.[10] The strong cationic exchange resin Amberlite IR-120 (Aldrich Chemical Co.) was rinsed with distilled water before use. D-Maltonolactone (maltlactone), was prepared according to literature procedures (iodine oxidation of the polysaccharide).[21,24] Dichloromethane and pentane were distilled from CaH, EtOH was distilled from Mg before use.

^{1}H and ^{13}C NMR were recorded at room temperature on a Bruker AC-200 spectrometer; solid state ^{13}C and ^{29}Si CPMAS NMR spectra were recorded on a Bruker AC-300 at 75.47 and 59.62 MHz, respectively. FTIR-ATR spectra were recorded on Bruker, Tensor 27. Electrospray mass spectra were recorded on a Micromass Quattro LC, triple quadruple MS. Thermogravimetric analyses were obtained using a Thermowaage Sta STA 409 at a heating rate of 3 °C min^{-1} from room temperature to 600 °C. X-ray photoelectron spectroscopy (XPS) was performed at Surface Interface Ontario (Toronto ON). The surfaces of the samples were analyzed using a Leybold Max 200 X-ray photoelectron spectrometer with a Mg Kα non-monochromatic X-ray source. The spot size used in all cases was 2 × 4 mm. Survey scans were performed from 0 to 1000 eV. Both low resolution and C(1s) high resolution analyses were performed. The raw data were analyzed and quantified using the software Specslab (Specs Gmbh, Berlin). Data were obtained at takeoff angles of 90°. Binding energies were referenced to the C(1s) signal for the carbon-silicon bond that was assigned a binding energy of 284.4 eV. The raw atomic% for Si(2p) and C(1s) signals were converted into ratios (Fig. 4). Elemental analyses were performed by Guelph Chemical Labs.

Preparation of silsesquioxane precursors

GLS: To a solution of D-gluconolactone (0.91 g, 5.2 mmol) in DMSO (10 mL) and EtOH (5 mL) was added 3-aminopropyltriethoxylsilane (1.11 g, 5.0 mmol). The mixture was stirred at 60 °C for 20 h. The solvents were evaporated under vacuum and the oil residue was dissolved in dichloromethane. Unreacted D-gluconolactone was filtered off, the filtrate was concentrated and added to a large amount of pentane. The white precipitate was collected and dried *in vacuo* to give **GLS** as a pale yellow solid, 1.83 g (92% yield). ^{1}H NMR (200.2 MHz, d_6-DMSO): δ 0.50 (m, 2H, $SiCH_2$), 1.12 (t, 9H, J = 6.98 Hz, $SiOCH^2CH^3$), 1.45 (m, br, 2H, $SiCH_2CH_2$), 3.04 (m, 2H, CH_2NHCO), 3.74 (q, J = 6.98 Hz, 6H, $SiOCH_2CH_3$), 3.40–5.32 (m, 11 H, glucose CH and CH_2, and OH), 7.61 (s, br, 1H, NHCO). ^{13}C NMR (50.3 MHz, d_6-DMSO): δ 7.8 ($SiCH_2$), 18.7–18.9 ($SiOCH_2CH_3$), 23.3 ($SiCH_2CH_2$), 41.5 (CH_2NHCO), 58.3 ($SiOCH_2CH_3$), 64.0, 70.7, 72.1, 74.2, 73.0 (glucose CH and CH_2), 172.9 (NHCO). FT-IR (KBr): 1646 cm^{-1} (ν(C=O)). MS-ESI (ES$^+$): 422.2 (M + Na, 100)$^+$, 400.2 (M + 1, 15)$^+$, 354 (5), 236 (18).

MLS: D-Maltonolactone was prepared using literature procedures in which maltose was oxidized with iodine.[24] To a solution of D-maltonolactone (0.75 g, 2.2 mmol) in DMSO (10 mL) and EtOH (5 mL) was added 3-aminopropyltriethoxysilane (0.44 g, 2.0 mmol). The mixture was stirred at 60 °C for 20 h. The solvents were evaporated under vacuum and oil residue was dissolved in dichloromethane. Unreacted D-maltonolactone was filtered off, the filtrate was concentrated and added to a large amount of pentane. The white precipitate was collected and dried in vacuo to give MLS as pale yellow solid, 0.98 g (87% yield). ^{1}H NMR (200.2 MHz, d_6-DMSO): δ 0.49 (m, br, 2H, $SiCH_2$), 1.08 (t, J = 6.96 Hz, 9H, $SiOCH_2CH_3$), 1.43 (m, br, 2H, $SiCH_2CH_2$), 3.70 (q, J = 6.96 Hz, 6H, $SiOCH_2CH_3$), 3.05–5.47 (m, 22 H, CH_2NHCO and maltose CH and CH_2, and OH), 7.60 (s, br, 1H, NHCO) ppm. ^{13}C NMR (50.3 MHz, d_6-DMSO): δ 7.8 ($SiCH_2$), 18.4–19.1 ($SiOCH_2CH_3$), 23.4 ($SiCH_2CH_2$), 41.3 (CH_2NHCO), 56.6 ($SiOCH_2CH_3$), 61.3, 63.4, 69.8, 72.5–73.8 (overlapped), 80.6, 101.4 (maltose CH and CH_2), 172.9 (NHCO) ppm. FT-IR (KBr): 1643 cm^{-1} (ν(C=O)). MS-ESI (ES$^+$): 584.3 (M + Na, 30)$^+$, 562.4 (M + 1, 20)$^+$.

Preparation of samples 1–10 and shrinkage measurements

All of the samples below were treated in the following way after gelation: fresh sol–gels were aged in a closed container at 5 °C for 20 h, then further aged at room temperature for 7 or 20 d. Aged hydrogels were washed with water 5 × 5 mL. This was done by soaking the whole aged gel (1 mL initial volume) in 5 mL water at room temperature for 4 h. The water was replaced 4 times, the last time the gel was kept over 8 h, for a total of 24 h. The gels were then allowed to dry at room temperature in an open container for 45 d. Shrinkage was recorded against the initial volumes of the sample sols on a v/v% basis (Figure 1).

Sample 1 (DGS gel). To a solution of DGS (240 mg, 1.1 mmol) in H_2O (0.50 mL) was added Tris buffer (0.50 mL, 50 mM, pH = 8.4). The mixture was left at room temperature to gel (Tables 2–4). After washing (see above) and drying for

45 d, the magnitude of shrinkage was recorded. Freeze drying gave a clear, colorless solid.

Sample 2 (DGS + sorbitol). To a solution of DGS (240 mg, 1.1 mmol) in H_2O (0.50 mL) was added sorbitol (60 mg, 0.33 mmol in 0.50 mL (50 mM, pH = 8.4) Tris buffer). The mixture was left at room temperature to gel (Tables 2–4). The hydrogel was aged at 4 °C for 20 h in a closed container, then further aged and dried in air at room temperature for 6 d. After washing (see above) and drying for 45 d, the magnitude of shrinkage was recorded. Shrinkage was then recorded. Freezing dried gave white powder.

Samples 3–10 (DGS + GLS (3–6) or + MLS (7–10). Prepared in a similar manner. The reaction conditions are listed in Table 2 and Table 4.

TGA analysis

Thermogravimetric analysis (TGA) was performed under air, with a flow rate of 50 cm^2 min^{-1}. The heating rate was 5 °C min^{-1} from room temperature to 750 °C. The TGA of unwashed samples is shown in Fig. 2. Washed samples were obtained by crushing the monolith; washing with deionized water for about 2 h with stirring using a magnetic stirring bar, at which point the water was removed by filtration. The washing and filtering was repeated 3 times, and in total, approximately 200 mL H_2O was used. A comparison of the drying of washed samples **1** and **4** is shown in Fig. 3. For the TGA of washed and freeze dried samples, shown in Table 4, the washed samples were further freeze dried at 0 °C for 20 h at 0.5–1 torr, after which the TGA was performed.

Monolith porosity

The nitrogen sorption isotherm, surface area and pore radius were measured with NOVA 2000 from Quantachrome Instruments. The samples were first prepared as were the TGA samples. The samples were then degassed with a final vacuum in the order of 10 millitorr (or less) for 5 h at 100 °C. BET surface area was calculated by the BET (Brunauer, Emmett and Teller) equation; the pore diameter from nitrogen adsorption–desorption isotherms was calculated by the Wheeler formula. All the data were calculated using the software provided with the instruments.

Acknowledgements

We acknowledge with gratitude the financial support of this research from MDS Sciex and the Natural Sciences and Engineering Research Council of Canada (NSERC). JDB holds the Canada Research Chair in Bioanalytical Chemistry. MAB thanks the Canada Council for the Arts for a Killam Fellowship (2003–2004).

References

1 C. J. Brinker and G. W. Scherer, *Sol–gel Science*, Academic Press, San Diego, 1990.
2 (*a*) D. S. Hage, *J. Chromatogr., B*, 1998, **715**, 3–38; (*b*) D. S. Hage, *Clin. Chem.*, 1999, **45**, 593–615; (*c*) M. G. Weller, *Fresenius' J. Anal. Chem.*, 2000, **366**, 635–645; (*d*) V. I. Muronetz, M. Sholukh and T. Korpela, *J. Biochem. Biophys. Methods*, 2001, **49**, 29–47; (*e*) T. Baczek and R. Kaliszan, *J. Biochem. Biophys. Methods*, 2001, **49**, 83–98; (*f*) R. R. Burgess and N. E. Thompson, *Curr. Opin. Biotechnol.*, 2002, **13**, 304–308.
3 (*a*) D. S. Hage, T. A. G. Noctor and I. W. Wainer, *J. Chromatogr., A*, 1995, **693**, 23–32; (*b*) H. Hofstetter, O. Hofstetter and V. Schurig, *J. Microcolumn Sep.*, 1998, **10**, 287–291; (*c*) O. Hofstetter, H. Lindstrom and H. Hofstetter, *Anal. Chem.*, 2002, **74**, 2119–2125; (*d*) L. Fitos, J. Visy and M. Simonyi, *J. Biochem. Biophys. Methods*, 2002, **54**, 71–84.
4 (*a*) Y. L. Hsieh, H. Wang, C. Elicone, J. Mark, S. A. Martin and F. Regnier, *Anal. Chem.*, 1996, **68**, 455–462; (*b*) C. Wang, R. Oleschuk, F. Ouchen, J. Li, P. Thibault and D. J. Harrison, *Rapid. Commun. Mass Spectrom.*, 2000, **14**, 1377–1383; (*c*) S. Wang and F. E. Regnier, *J. Chromatogr., A*, 2001, **913**, 429–436; (*d*) D. S. Peterson, T. Rohr, F. Svec and J. M. J. Frechet, *J. Proteome Res.*, 2002, **1**, 563–568; (*e*) D. S. Peterson, T. Rohr, F. Svec and J. M. J. Frechet, *Anal. Chem.*, 2002, **74**, 4081–4088; (*f*) G. W. Slysz and D. C. Schriemer, *Rapid Commun. Mass Spectrom.*, 2003, **17**, 1044–1050.
5 D. Prazeres, F. Miguel and J. M. S. Cabral, in *Multiphase Bioreactor Design*, ed. J. M. S. Cabral, M. Mota and J. Tramper, Taylor & Francis Ltd., London, UK, 2001, pp. 135–180.
6 (*a*) D. C. Schriemer, D. R. Bundle, L. Li and O. Hindsgaul, *Angew. Chem., Int. Ed.*, 1998, **37**, 3383; (*b*) B. Zhang, M. M. Palcic, D. C. Schriemer, G. Alvarez-Manilla, M. Pierce and O. Hindsgaul, *Anal. Biochem.*, 2001, **299**, 173–182.
7 (*a*) M. T. Baynham, S. Patel, R. Moaddel and I. W. Wainer, *J. Chromatogr., B*, 2002, **772**, 155–161; (*b*) R. Moaddel, L. Lu, M. Baynham and I. W. Wainer, *J. Chromatogr., B*, 2002, **768**, 41–53; (*c*) R. Moaddel, J.-F. Cloix, G. Ertem and I. W. Wainer, *Pharm. Res.*, 2002, **19**, 104–107; (*d*) R. Moaddel and I. W. Wainer, *J. Pharm. Biomed. Anal.*, 2003, **30**, 1715–1724.
8 I. Gill and A. Ballesteros, *J. Am. Chem. Soc.*, 1998, **120**, 8587.
9 (*a*) M. A. Brook, J. D. Brennan and Y. Chen, *Polyol-Modified Silanes as Precursors for Silica*, US Patent Application, 60/384084, McMaster University; (*b*) Y. Chen, J. D. Brennan and M. A. Brook, *Controlled Shrinkage Sol–Gel Silsesquioxane Precursors*, US Patent Application 60/405308, McMaster University.
10 (*a*) M. A. Brook, Y. Chen, K. Guo, Z. Zhang and J. D. Brennan, *J. Sol-Gel Sci. Technol.*, 2004, **31**, 343–348; (*b*) M. A. Brook, Y. Chen, Z. Zhang and J. D. Brennan, *J. Mater. Chem.*, 2004, **14**, 1469–1479.
11 T. R. Besanger, Y. Chen, A. K. Deisingh, R. Hodgson, W. Jin, S. Mayer, M. A. Brook and J. D. Brennan, *Anal. Chem.*, 2003, **75**, 2382–2391.
12 T. Arakawa and S. N. Timasheff, *Biochemistry*, 1982, **21**, 6536.
13 (*a*) J. A. Cruz-Aguado, Y. Chen, Z. Zhang, M. A. Brook and J. D. Brennan, *Anal. Chem.*, 2004, **76**, 4182–4188; (*b*) J. A. Cruz-Aguado, Y. Chen, Z. Zhang, N. H. Elowe, M. A. Brook and J. D. Brennan, *J. Am. Chem. Soc.*, 2004, **126**, 6878–6879.
14 R. H. Baney, M. Itoh, A. Sakakibara and T. Suzuki, *Chem. Rev.*, 1995, **95**, 1409.
15 (*a*) For other reviews, see: M. G. Voronkov and V. I. Lavrent'yev, *Top. Curr. Chem.*, 1982, **102**, 199; (*b*) J. D. Lichtenhan, in *Polymeric Materials Encyclopedia: Synthesis, Properties and Applications – Silsesquioxane-Based Polymers*, ed. J. C. Salsmone, CRC Press, Boca Raton, Florida, 1996, p. 7768.
16 E. P. Plueddemann, *Silane Coupling Agents, 2nd ed.*, Plenum, New York, 1991.
17 (*a*) D. A. Loy, A. Straumanis, D. A. Schneider, B. Mather, A. Sanchez, C. R. Baugher and K. J. Shea, *Polym. Prepr.*, 2004, **45**, 591; (*b*) E. R. Pohl and F. O. Osterholz, in *Silanes, Surfaces and Interfaces, Vol. 1*, ed. D. E. Leyden, Gordon and Breach, Amsterdam, 1986, p. 481.
18 (*a*) Y. Chujo and T. Saegusa, *Adv. Polym. Sci.*, 1992, **100**, 11; (*b*) Y. Schubert, in *Organically Modified Silica Aerogels from RSi(OR')3/Si(OR')4 Mixtures in Tailor-Made Silicon-Oxygen Compounds*, ed. R. Corriu and P. Jutzi, Vieweg, Wiesbaden, Germany, 1996, p. 263 (from a workshop at the University of Bielefeld, 1995).
19 It should be noted that previous work has produced sugar modified silica by first modifying a silica surface with a coupling agent, and

then adding a saccharide moiety, or directly using saccharidic coupling agents to modify preexisting silica.[21] This is distinct from the "one-shot" use of saccharidic trifunctional silanes as siliceous monolith precursors. These silanes can be both internal and external constituents of the produced gel, which modify both bulk and surface properties.

20 (*a*) M. Kanno and S. Kusakaishi, Japanese Patent 3046964, Tohoku Munekata K. K., Japan, 1999; (*b*) Japanese Patent Application 79-169422, Showa Denko K. K., Japan, 1979; (*c*) T. Uehara and Y. Tajima, Japanese Patent Application 92-264622, Sekisui Chemical Co Ltd, Japan, 1992.

21 Gluconamides: (*a*) R. J. DePasquale and M. E. Wilson, US Patent 4591652, SCM Corp., USA, 1986; (*b*) M. Haupt, S. Knaus, T. Rohr and H. Gruber, *J. Macromol. Sci., Pure Appl. Chem.*, 2000, **A37**, 323. A related compound, the maltopentaose-modified silane: N. Enomoto, S. Furukawa, Y. Ogasawara, H. Akano, Y. Kawamura, E. Yashima and Y. Okamoto, *Anal. Chem.*, 1996, **68**, 2798.

22 X. Sui, J. A. Cruz-Aguado, Y. Chen, Z. Zhang, M. A. Brook and J. D. Brennan, *Chem. Mater.*, 2005, **17**, 1174–1182.

23 We note that the same methodology has been applied to the preparation of dextran-modified silanes. However, the curing chemistry of these materials is more complex, much slower, and not discussed further in this paper.

24 (*a*) K. Hamshimoto, S. Imanishi, M. Okada and H. Sumitomo, *J. Polym. Sci., Polym. Chem. Ed.*, 1991, **29**, 1271; (*b*) T. Zhang and R. E. Marchant, *Macromolecules*, 1994, **27**, 7302.

25 We have compared the shrinkage of all samples at least up to 57 d. Little shrinkage occurs after this time, as long as the conditions are held the same (*e.g.*, under water, in air, *etc.*). As an example, unwashed DGS gels underwent no further shrinkage from 57 d to two years when aged in air in an open container.

26 (*a*) J. A. Hockey, *Chem. Ind.*, 1965, 57; (*b*) R. K. Iler, *The Chemistry of Silica*, John Wiley & Sons, New York, 1979; (*c*) E. F. Vansant, P. Van Der Voort and K. C. Vrancken, *Characterization and chemical modification of the silica surface*, Elsevier, Amsterdam, 1995.

27 (*a*) S. H. Phillips, T. S. Haddad and S. J. Tomczak, *Curr. Opin. Solid State Mater. Sci.*, 2004, **8**, 21–29; (*b*) F. J. Feher, R. Terroba, R.-Z. Jin, S. Lucker, F. Nguyen, R. Brutchey and K. D. Wyndham, *Mater. Res. Soc. Symp. Proc.*, 2001, **628** (Organic/Inorganic Hybrid Materials), CC2.1.1–CC2.1.6; (*c*) J. J. Schwab and J. D. Lichtenhan, *Appl. Organomet. Chem.*, 1998, **12**, 707–713.

28 (*a*) Y. Koide, Q. Wang, J. Cui, D. D. Benson and T. J. Marks, *J. Am. Chem. Soc.*, 2000, **122**, 11266–11267; (*b*) T. J. Marks, Ji. Cui, J. E. Malinsky, Q. Wang, G. E. Jabbour, S. E. Shaheen, J. D. Anderson, P. A. Lee, A. G. Richter, B. Kippelen, P. Dutta, N. Peyghambarian and N. R. Armstrong, *Polym. Prepr.*, 1999, **40**, 2, 1196–1197.

29 Many such patents exist. See, for example: R. P. Boisvert, G. T. Burns, T. C.-S. Chao, D. E. Katsoulis and S. K. Sarmah, US Patent 5972512, Dow Corning, 1999.

30 (*a*) D. Belton, G. Paine, S. V. Patwardhan and C. C. Perry, *J. Mater. Chem.*, 2004, **14**, 2231–2241; (*b*) C. C. Perry, *Rev. Mineral. Geochem.*, 2003, **54**, 291–327; (*c*) C. C. Perry and T. Keeling-Tucker, *J. Biol. Inorg. Chem.*, 2000, **5**, 537–550.

31 (*a*) S. D. Kinrade, R. J. Hamilton, A. S. Schach and C. T. G. Knight, *J. Chem. Soc., Dalton Trans.*, 2001, 961; (*b*) S. D. Kinrade, K. J. Maa, A. S. Schach, T. A. Sloan and C. T. G. Knight, *J. Chem. Soc., Dalton Trans.*, 1999, 3149.

32 (*a*) D. Tleugabulova, A. M. Duft, Z. Zhang, Y. Chen, M. A. Brook and J. D. Brennan, *Langmuir*, 2004, **20**, 5924–5932; (*b*) D. Tleugabulova, Z. Zhang, Y. Chen, M. A. Brook and J. D. Brennan, *Langmuir*, 2004, **20**, 848–854.

33 (*a*) E. R. Pohl and F. D. Osterholtz, *Polym. Sci. Technol.*, 1985, **27**, 157; (*b*) Y. Sugahara, S. Okada, S. Sato, K. Kuroda and C. Kato, *J. Non-Cryst. Solids*, 1994, **167**, 21; (*c*) K. A. Smith, *Macromolecules*, 1987, **20**, 2514; (*d*) F. D. Osterholtz and E. R. Pohl, *J. Adhes. Sci. Technol.*, 1992, **6**, 127.

34 D. W. Bolen, *Methods*, 2004, **34**, 312–322.

35 D. K. Eggers and J. S. Valentine, *J. Mol. Biol.*, 2001, **314**, 911–922.

36 R. J. Hodgson, Y. Chen, Z. Zhang, D. Tleugabulova, H. Long, X. Zhao, M. Organ, M. A. Brook and J. D. Brennan, *Anal. Chem.*, 2004, **76**, 2780–2790.